Ferritin Effect on the Transverse Relaxation of Water: NMR Microscopy at 9.4 T

Ziv Gottesfeld, Michal Neeman

Accumulation of ferritin, the iron storage protein, has been linked recently to aging and a number of pathologies. Noninvasive detection of iron storage by MRI relies on its extremely strong effect on water relaxation. The aim of this article is to characterize the effect of ferritin on transverse water relaxation in a high magnetic field, using an imaging Carr-Purcell Meiboom-Gill (CPMG) preparation sequence. Ferritin-induced water relaxation showed quadratic dependence on the iron loading factor, implying a paramagnetic mechanism. However, an additional zero order term was found, that could be due to the initial stages of the iron core loading. Significant enhancement of ferritin contrast was obtained at very short τ_{CPMG} durations. This approach for enhancing ferritin contrast was demonstrated by NMR microscopy of ferritin-injected *Xenopus* oocytes, thus showing the feasibility of ferritin detection in a high magnetic field, even in systems with short transverse relaxation.

Key words: NMR microscopy; ferritin; iron loading; *Xenopus* oocyte.

INTRODUCTION

Ferritin is a large protein (~130 Å in diameter), whose major role is to store and detoxify intracellular iron (1, 2). It consists of a protein shell of 24 subunits (weighing a total of 447 kd) arranged in 4–3-2 symmetry, forming an inner cavity of approximately 80 Å, which can accommodate up to 4500 atoms of iron in the form of hydrous ferric oxide (2). The possible association between elevated levels of brain iron in aging and certain pathologies (e.g., see refs. 3 and 4), led to a number of recent MRI studies of the correlation between transverse relaxation in brain images and iron content (see refs. 5–7 and references cited therein).

Low field NMR studies showed that ferritin had a very significant effect on the relaxation transverse of water (8), as well as an unusual nuclear magnetic relaxation dispersion (NMRD) profile (9). The transverse relaxivity of ferritin (R_2), measured at 20 MHz, was more than three orders of magnitude greater than that expected according to the principles of outer sphere relaxation theory (8). In addition, a linear dependence of the transverse relaxation rate on the strength of the magnetic field (up to 60 MHz) was observed, rather than the expected quadratic dependence (9). These unusual magnetic properties of ferritin have been previously associated with superparamagnetism (10). One possible explanation may be that the external shape of the iron core, imposed stress, or the crystal structure itself varies with the loading factor and affects magnetic properties. Another model that may explain ferritin's effect on T_2 relaxivity is the one that proposes that ferromagnetic domains are formed in the initial stages of iron loading due to imperfect oxidation of the ferrous ions, followed by a much smaller paramagnetic contribution as the loading factor is increased. The effect of the ferritin loading factor on transverse relaxivity ($R_2 = 1/T_2$) has not been determined.

In a high magnetic field, the secular transverse relaxation term dominates. Therefore, the contribution of a magnetized relaxation agent to transverse relaxation can be approximated by the following equation (10):

$$R_2 = 16/135\, f(\delta\omega)^2 \qquad [1]$$

where f is the volume fraction of relaxation agent and δ is the field inhomogeneity at the surface. The field inhomogeneity at the surface of a magnetized sphere is proportional to its total magnetization:

$$\delta\omega = \mu\, \gamma_l / R^3 \qquad [2]$$

where μ is magnetization, γ the proton gyromagnetic ration, and R the radius of the sphere. In a paramagnetic model, total magnetization is, in turn, proportional to the number of magnetic particles contained within the sphere. Thus, the transverse relaxation contribution of a magnetized relaxation agent, such as ferritin, is expected to be quadratically dependent on the loading factor.

For the longitudinal relaxation of ferritin, it has been shown that relaxation enhancement saturates after the loading of 24 iron ions per protein; i.e., the bulk of the iron core offers little additional contribution (8). T_1 measurements at very low field (0.02–20 MHz) showed that iron ions at the binding sites of the ferritin protein contribute to relaxation through direct dipolar interaction with water protons (8). This contribution is on the order of 0.2 s^{-1}/mg/ml, caused by 6–8 ions per protein. In a high field, the contribution to transverse relaxation through such a mechanism is expected to be small, compared to that of outer sphere mechanisms, such as the diffusion of water protons past the ferritin complex.

Enhancement of the effect of ferritin in MRI can be obtained if competing relaxation mechanisms in the tissue are refocused. The major components that shorten the apparent T_2 in tissues arise from water diffusion through regions with varying bulk magnetic susceptibility and from the interaction of water with macromolecules. The former mechanism can be effectively refocused by application of a Carr-Purcell-Meiboom-Gill

MRM 35:514–520 (1996)

From the Department of Hormone Research, Weizmann Institute of Science, Rehovot, Israel.

Address correspondence to: Dr. Michal Neeman, Department of Hormone Research, Weizmann Institute of Science, Rehovot 76100, Israel.

Received May 17, 1995; revised September 13, 1995; accepted October 13, 1995.

M.N. is the incumbent of the Dr. Phil Gold Career Development Chair in Cancer Research.

0740-3194/96 $3.00

Copyright © 1996 by Williams & Wilkins
All rights of reproduction in any form reserved.

(CPMG) sequence, with short interecho duration (τ_{CPMG}) relative to the rate of diffusion, i.e., in the millisecond range. Refocusing of the second mechanism can be expected in the very short τ_{CPMG} regime (11). In this range, spins do not dephase significantly between refocusing pulses and, hence, may be locked by the effective refocusing fields of the pulses. The relaxation measured at a very short τ_{CPMG} sequence is, therefore, approaching $T_1\rho$, the longitudinal relaxation in the rotating frame (11).

In this study we measured the effect of application of a CPMG preparation with varying τ_{CPMG} on the contrast provided by ferritin. The effectiveness of this approach was evaluated by NMR microscopy of *Xenopus* oocytes, a system with an extremely short T_2 relaxation time, which is on the order of 15 ms (12–14).

MATERIALS AND METHODS

Iron Loading

Apoferritin solutions (Sigma Chemicals, St. Louis, MO) at various concentrations (0.008 μM to 0.5 μM in 0.1 *M* Hepes buffer, pH 7.0, final volume 20 ml) were incubated (4°C, 24 h) with 0.3 m*M* ferrous ammonium sulfate. Solutions were then centrifuged (15 min, at 10,000 g), and the supernatants were dialyzed twice against 4 liters of double-distilled water for 24 h. Samples were stored at 4°C for NMR measurements and determination of protein and iron content. The loading factor obtained was determined as reported previously (1): ferritin samples were incubated in 1 *M* acetic acid, 0.5% 3-(2-pyridyl)-5,6-*bis*(4-phenylsulfonic acid)-1,2,4-triazine, boiled for 60 min, and the absorbance was read at 565 nm. Ferrous ammonium sulfate was used as standard. Protein concentrations were determined with Bradford reagent, using bovine serum albumin (BSA) as standard (15). All ferritin concentrations are expressed in milligrams of protein per milliliter, as determined by the Bradford assay.

Preparation of *Xenopus* Oocytes

Oocytes were isolated and cultured as described previously (15, 16). Ferritin (cadmium-free, 1830 Fe/protein, Boehringer Mannheim, Mannheim, Germany) and apoferritin (Sigma) at a protein concentration of 20 mg/ml, were microinjected into oocytes at the midline. The injected volume was 50 nl, resulting in a final protein concentration within the oocyte of approximately 1 mg/ml. NMR experiments were conducted 24 h postinjection at room temperature (23°C). Ferritin-injected oocytes were placed in culture medium (15, 16) in a 5-mm NMR tube at one side of a divider, and apoferritin-injected oocytes were placed at the other side (2–3 oocytes for each treatment). The oocyte nucleus was apparent in all NMR images, as reported previously (12–14). Regions of interest from the animal pole (cytoplasm from the side of the nucleus) and the vegetal pole of each oocyte were selected, relative to the position of the nucleus.

NMR Measurements

Experiments were performed on a Bruker AMX 400 spectrometer, equipped with microscopy accessories and using actively shielded magnetic field gradients, as well as a 5-mm Helmholtz RF coil. Spectroscopic measurements of transverse relaxation were obtained, using a modified CPMG sequence, in which crusher gradients (5 G/cm, 3 ms) were applied on both sides of the last refocusing pulse. The time to echo from the last of the 180° pulse series was 12.1 ms. The CPMG preparation included a $90°_x$ pulse, followed by a series of τ_{CPMG} -$180°_y$ -τ_{CPMG}. Total echo time (*TE*) was varied by changing the number of τ- $180°_y$ - τ loops. Ten echo times (20–200% of T_2) were collected for each sample. The acquisition parameters were: spectral width of 4 kHz, *TR* of 20 s, and pulse durations of 7 and 13.5 μs for the $90°_x$ and $180°_y$ pulses, respectively.

Determination of T_2 values from NMR microscopy was done, using a similar CPMG-preparation imaging sequence. A hard $90°_x$ pulse was followed by a train of τ_{CPMG} -hard $180°_y$ pulse- τ_{CPMG}, ending with a single-slice selective 2-ms sinc refocusing pulse. The time to echo from the last of the CPMG series was 9.12 ms. Total echo time (*TE*) was varied by changing the number of τ_{CPMG} - $180°_y$ - τ_{CPMG} loops. Pixels (128 × 64) were acquired with a frequency-encoding gradient of 19.6 G/cm and in plane resolution of 92 × 46 μm. Sample temperature was maintained, using the Bruker temperature control unit. Sample heating, due to the τ_{CPMG} sequence, was measured on a BSA-ferritin solution, using an external thermocouple. Heating, measured 1 s after the RF pulse train, was less than 0.1°C in all cases.

Data Processing

Data was analyzed on a Personal Iris computer (Silicon Graphics, Mountain View, CA), using software packages MATLAB (The Mathworks, Natick, MA) and IMAGE (New Methods Research, Syracuse, NY). Relaxation curves were fit to single or biexponential model by a nonlinear least square algorithm. Pixel by pixel optimizations were performed for images.

RESULTS

Effect of Ferritin Iron Loading on the Transverse Relaxation of Water

Ferritin samples with different iron loading were prepared as described previously (1). Water relaxation was measured, using a CPMG preparation sequence with τ_{CPMG} of 0.5 ms and was analyzed by single exponential least square optimization (Fig. 1). The specific relaxivity due to the iron core of ferritin (R_{2core}) was determined from the difference of relaxation in each ferritin sample from the relaxation of an apoferritin sample, using the following relation:

$$R_{2core} = R_{2fer}/C_{fer} - R_{2apo}/C_{apo} \quad [3]$$

where R_{2fer} and R_{2apo} are the experimental relaxation rates (s^{-1}) of ferritin and apoferritin samples, and C_{fer} and C_{apo} are the concentrations (milligrams of protein per milliliter) of the ferritin and apoferritin samples, respectively.

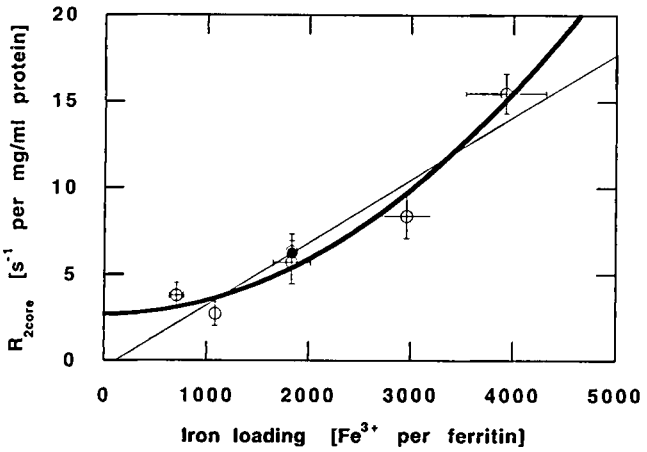

FIG. 1. The effect of ferritin iron loading on transverse relaxivity. Ferritin, with loading factor ranging from 700 to 4000 irons per protein, was prepared as described in Materials and Methods. Relaxivity due to the iron core of ferritin was found, using a CPMG spin-echo sequence, as described in Results, in Eq. [3]. The dependence of relaxivity on the loading factor was modeled by the sum of a zero order and a second order term (solid bold line). The data point, marked by a solid circle, was obtained from commercial ferritin (Boehringer Mannheim, Mannheim, Germany). A linear regression (thin line) gave a worse fit to the data.

The specific transverse relaxivity R_{2core} was dependent on the loading factor (Fig. 1). A good fit was obtained for a sum of a quadratic term and a zero order offset. Thus, the effect of iron loading on the specific relaxivity was fit to the following polynomial:

$$R_{2core} = A_0 + A_2 L^2 \quad [4]$$

where L denotes the loading factor. Best fit was found for $A_0 = 2.7$ (± 0.5) [s^{-1}/mg/ml protein] and $A_2 = 8$ (± 0.9) * 10^{-7} [s^{-1} × (loading factor)$^{-2}$/mg/ml of protein]; (R^2 = 0.96, χ^2 = 4.67; Fig. 1, bold line). Addition of a linear term did not significantly improve the fit. A linear regression gave a worse reproduction of the experimental data (R^2 = 0.90, χ^2 = 10.40; Fig. 1, thin line).

The second order quadratic term ($A_2 = 8 \times 10^{-7}$ [s^{-1} × (loading factor)$^{-2}$/mg/ml protein]) can represent the paramagnetic properties of the iron core (as outlined in the Introduction). The zero order term ($A_0 = 2.7$ [s^{-1}/mg/ml protein]), however, could not be explained by paramagnetism. This term was significant and could not be accounted for by experimental errors in loading factor, protein concentration, or relaxation rate measurement. The error in determination of the iron loading factor was less than 10%, and relaxivity errors were less than 20%. Contribution of free iron to the zero order term was also ruled out. The amount of iron ions that remained in ferritin solutions after dialysis was less than 1% of the initial amount, i.e., less than 3 μM at the highest loading factor. Iron self-oxidation was measured by incubation of ferrous ammonium sulfate (30 μM, 72 h) at room temperature. The contribution to transverse relaxivity after dilution to 3 μM was under 0.04 s^{-1}. For the lower loading factors, which are the main determinants of the zero order term, the contribution would be about five times smaller. Thus, according to the data presented here, the zero order term stems from a true property of ferritin at low iron loading.

Optimization of Ferritin-induced Contrast in High Field ^{1}H MRI

Transverse relaxation maps of water were reconstructed from images of phantoms containing BSA and horse spleen ferritin solutions in a standard 5-mm tube (4.20 mm ID), with an external concentric reference (1.25 mm ID) containing the BSA solution. The transverse decay curves of four solutions, including water, BSA (50 mg/ml), BSA (50 mg/ml) + ferritin (0.02 mg/ml), and BSA (50 mg/ml) + ferritin (0.1 mg/ml), were well fit to a monoexponential model at all τ_{CPMG} values. Reconstructed transverse relaxation maps showed a significantly larger difference between ferritin and BSA relaxation at τ_{CPMG} of 0.1 ms than at τ_{CPMG} of 1 ms (Fig. 2). Quantitative determination of the effect of τ_{CPMG} on ferritin-induced contrast was, therefore, carried out. Analysis of the transverse relaxation rate of the BSA and the two BSA + ferritin solutions showed a similar dependence on τ_{CPMG} (Fig. 3A). In these solutions, the relaxation rate rose by 0.8 s^{-1} between τ_{CPMG} of 50 μs and τ_{CPMG} of 1 ms, where a plateau was approached (Fig. 3A). The relaxation rate of tap water changed by only 0.161 s^{-1} between these τ_{CPMG} values. Thus, the longer T_2 time at short τ_{CPMG}, as well as the enhanced ferritin-induced contrast, can be attributed to refocusing of a component of relaxation associated with BSA.

Analysis of the effects of τ_{CPMG} on water relaxation in BSA solutions can be done in analogy with the spin-lock effect on water relaxation (see ref. 11; Fig. 3B). Indeed, the resulting NMRD profile was well fit to a spin-lock model of the type:

$$1/T_{1\rho} = R + A\,\tau/[1 + 4\,\tau^2\omega^2] \quad [5]$$

where R is the relaxation component that is not affected by the RF frequency ω. The pulse frequency ω is given by $\omega = \Pi/2\ \tau_{CPMG}$, A is the component that is affected by ω,

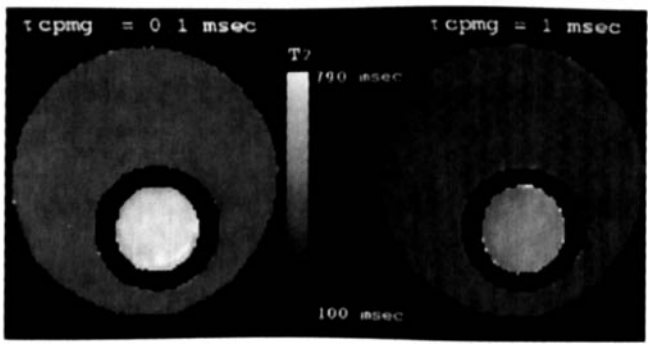

FIG. 2. T_2 maps of ferritin-BSA phantoms. Ferritin-BSA solutions (0.02 or 0.1 mg/ml ferritin and 50 mg/ml BSA) were placed in a standard 5-mm NMR tube (4.20 mm id). Concentric external BSA (50 mg/ml) reference was placed in a 1.25-mm tube. T_2 maps were reconstructed from data sets of 4 to 5 images, measured using a CPMG preparation imaging sequence. Imaging parameters were: TR = 4 s, slice thickness 0.7 mm, 128 * 64 pixels, with in-plane resolution of 92 μm * 46 μm. Slice gradient was 10 G/cm, and frequency-encoding gradient 19.6 G/cm. (Left) τ_{CPMG} = 0.1 ms. (Right) τ_{CPMG} = 1 ms.

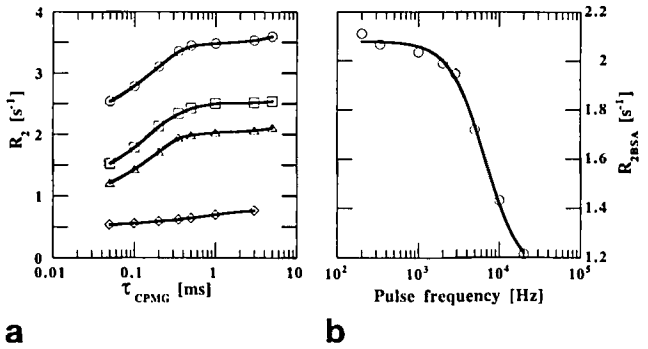

FIG. 3. The effects of τ_{CPMG} on transverse relaxation rates. (a) Mean transverse relaxation rates obtained from reconstructed T_2 maps of tap water (diamonds), BSA (triangles), and ferritin-BSA (squares, 0.02 mg/ml ferritin; circles, 0.1 mg/ml ferritin). Relaxation rate of BSA and ferritin-BSA rose by about 0.8 s^{-1} from τ_{CPMG} of 50 μs to the plateau at τ_{CPMG} of 1 ms. Water relaxation rate (diamonds) rose by only 0.16 s^{-1} in this τ_{CPMG} range. (b) NMRD profile of BSA. BSA relaxation rates (circles) were modeled by a spin-lock NMRD profile of the type: $1/T_1\rho = R + A\,\tau/[1 + 4\,\tau^2\omega^2]$ (solid line); where ω is the refocusing pulse frequency in radial frequency units. The parameters for best fit were: r = 1.12 s^{-1}, $A = 0.079 \cdot 10^6$ s^2, $\tau = 12 \cdot 10^{-6}$ s.

and τ is the typical correlation time of the relaxation mechanism. Fitting the BSA data to this model yielded a correlation time τ of 12 ($\pm$1) μs, r = 1.12 s^{-1} and $A = 0.079 \times 10^6$ s^2 (Fig. 3B).

In contrast with the findings for BSA, ferritin relaxivity was not affected by the τ_{CPMG} duration (Fig. 4A). Ferritin contrast (FC) in these samples was defined as the normalized difference in intensities between the BSA and ferritin solutions:

$$FC = \exp(-R_{2BSA} * TE) - \exp(-R_{2fer} * TE) \qquad [6]$$

The maximal contrast will be reached at an optimal echo time (TE_{opt}) given by:

$$TE_{opt} = [\ln(R_{2FER}/R_{2BSA})]/(R_{2FER} - R_{2BSA}) \qquad [7]$$

The contrast at optimal TE (for the 0.1 mg/ml of ferritin solution) was 35.2% higher at the shortest τ_{CPMG} = 50 μs relative to the plateau at $\tau_{CPMG} > 1$ ms (Fig. 4B).

The uniformity of signal intensity ($\pm$5%) in the raw images, as well as in the reconstructed T_2 and spin density (A_0) maps, enables us to determine from these data sets the spin density and T_2 values for specific regions of interest. This is particularly important in the study of biological samples, as will be shown below.

Determination of Transverse Relaxation of Water in *Xenopus* Oocytes

The results of ferritin-induced contrast in solution were challenged in the *Xenopus* oocyte, which is known to have an extremely short cytoplasmic T_2 of approximately 15 ms (12, 13). Imaging was conducted at a τ_{CPMG} of 100 μs, which provided the best signal-to-noise ratio in our system. The animal pole, vegetal pole, and the nucleus could be distinguished in the oocytes (Fig. 5A). At minimal echo time (9.12 ms), the mean signal intensity in the animal pole was 1.5 ($\pm$ 0.2)-fold larger than that of the vegetal pole (N = 17), whereas the nucleus intensity was 2.1 ($\pm$ 0.5)-fold that of vegetal pole ($P < 0.05$, Student's t test). At longer echo times, the difference in intensity between the animal and vegetal poles was smaller, whereas the nucleus remained brighter. Relaxation curves of water in the animal and vegetal poles displayed a distinct multiexponential behavior (Fig. 5B). Previous studies of tissue relaxation times reported three major components on the order of 5, 50, and 140 ms (11). Due to signal-to-noise ratio, limitations the data presented here could not support a model beyond biexponential decay (Table 1).

$$I = C_a * \exp(-TE/T_{2a}) + C_b * \exp(-TE/T_{2b}) \qquad [8]$$

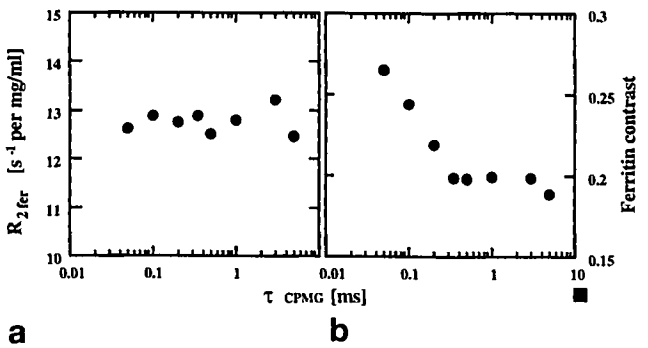

FIG. 4. Optimization of ferritin contrast. (a) Ferritin relaxation rate per milligram per ml of protein as a function of τ_{CPMG}. Specific ferritin relaxivity was calculated, using the relaxation data of two ferritin concentrations (0.1 and 0.02 mg/ml of protein). No significant τ_{CPMG} dependence was found. The mean relaxivity of this ferritin sample (Sigma, St. Louis, MO) was (12.76 $\pm$ 0.24) s^{-1}/mg/ml protein. (b) Dependence of the maximal ferritin-induced contrast on τ_{CPMG}. Contrast at optimal TE was calculated from the relaxation rates of ferritin (0.1 mg/ml). Optimal TE is the echo time, yielding the largest contrast between ferritin and BSA. The maximal contrast was more than 35% higher at 50 μs than at the plateau region.

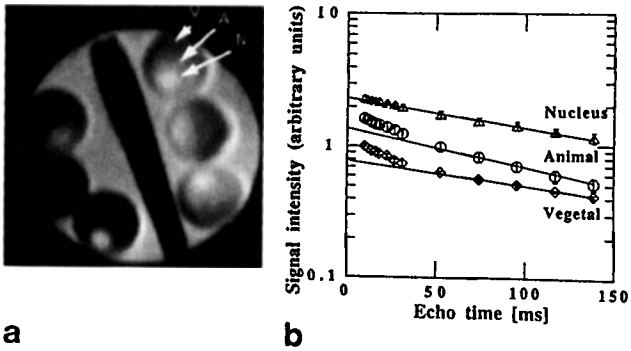

FIG. 5. NMR microscopy of ferritin-contrast in *Xenopus* oocytes. (a) *Xenopus* oocytes were imaged, using a CPMG preparation sequence with τ_{CPMG} duration of 100 μs, TR of 3.5 s, 4 averages, slice thickness of 0.6 mm, echo time of 10 ms, and 96 $\times$ 46 μm in-plane resolution. Ferritin-injected oocytes (50 nl, 20 mg/ml) are on the left side of the divider, and apoferritin-injected oocytes are on the right side. The lower signal intensity of ferritin-injected oocytes is apparent even at short echo time. A = animal pole, V = vegetal pole, N = nucleus. (b) Transverse magnetization decay curves of the animal pole, vegetal pole, and nucleus (mean of five untreated oocytes). Dashed lines show a single exponential analysis, using the last data points.

Table 1
Biexponential Relaxation of Water in Ferritin- and Apoferritin-injected *Xenopus* Oocytes

	Injection	C_a[a,b]	T_{2a}[a]	C_b[a,b]	T_{2b}[a]	C_b/C_a
Animal	Apoferritin	0.36 ± 0.05	18 ± 1	0.64 ± 0.05	80 ± 12	1.7 ± 0.3
pole	Ferritin	0.42 ± 0.13	12 ± 2[c]	0.35 ± 0.06[c]	116 ± 23[c]	0.8 ± 0.3[c]
Vegetal	Apoferritin	0.22 ± 0.05	17 ± 3	0.47 ± 0.04	113 ± 11	2.1 ± 0.5
pole	Ferritin	0.23 ± 0.08	11 ± 4[c]	0.33 ± 0.05[c]	119 ± 15	1.4 ± 0.5[c]
Nucleus	Apoferritin	0.33 ± 0.07	25 ± 1	0.87 ± 0.03	113 ± 9	2.6 ± 0.6
	Ferritin	0.37 ± 0.02	14 ± 4[c]	0.78 ± 0.05	126 ± 28	2.1 ± 0.2

The mean ± SD of 17 oocytes is reported here.
[a] Bioexponential curve fits were obtained pixel by pixel for each data set. The values of $T_{2a,b}$ and C_{ab} were determined for each region of interest in each oocyte from the corresponding reconstructed maps.
[b] Normalized coefficients ($C_a + C_b = 1$ in the animal pole of apoferritin-injected oocytes).
[c] Significant difference between apoferritin and ferritin injected oocytes (p value < 0.05 Student t-test).

where C_a and C_b are the partial contributions to each decay constant and T_{2a} and T_{2b} are the corresponding relaxation times. In control, noninjected oocytes and in oocytes injected with apoferritin, the two relaxation times were 18 and 80 ms for the animal pole, 17 and 113 ms for the vegetal pole, and 25 and 113 ms for the nucleus (Table 1). Bioexponential curve fits were obtained pixel by pixel for each data set. The values of $T_{2a,b}$ and C_{ab} (mean ± SD of 17 oocytes) were determined for each region of interest in each oocyte from the corresponding reconstructed maps.

Ferritin-induced Contrast in *Xenopus* Oocyte

^{1}H NMR signal intensity of oocytes injected with ferritin was significantly lower in all regions of interest relative to control uninjected oocytes or oocytes injected with apoferritin (Figs. 5A and 6A, respectively). This effect was due to the iron core, as no significant intensity difference was observed between apoferritin-injected and uninjected oocytes. Ferritin contrast, namely, the difference between signal intensity of apoferritin- and ferritin-injected oocytes, was maximal at the minimal echo time for both the animal and vegetal poles (Fig. 6B). The mean maximal drop in signal intensity caused by ferritin was 37% (±6) for the animal pole and 32% (±14) for the vegetal pole (three experiments, six apoferritin- and eight ferritin-injected oocytes). Ferritin contrast in the nucleus varied between 13 and 66%, probably due to partial volume effects.

Using biexponential analysis, T_2 components of about 20 and 100 ms were found for the cytoplasm of apoferritin-injected oocytes (Table 1). Ferritin-injected oocytes displayed a significant drop of about 6 ms in the short T_{2a} cytoplasmic component. The long T_{2b} component was not significantly affected in the vegetal pole and showed a slight increase in the animal pole. Ferritin-injected oocytes showed a marked increase in C_a, relative to C_b. Apparent cytoplasmic spin density ($C_a + C_b$) was signif-

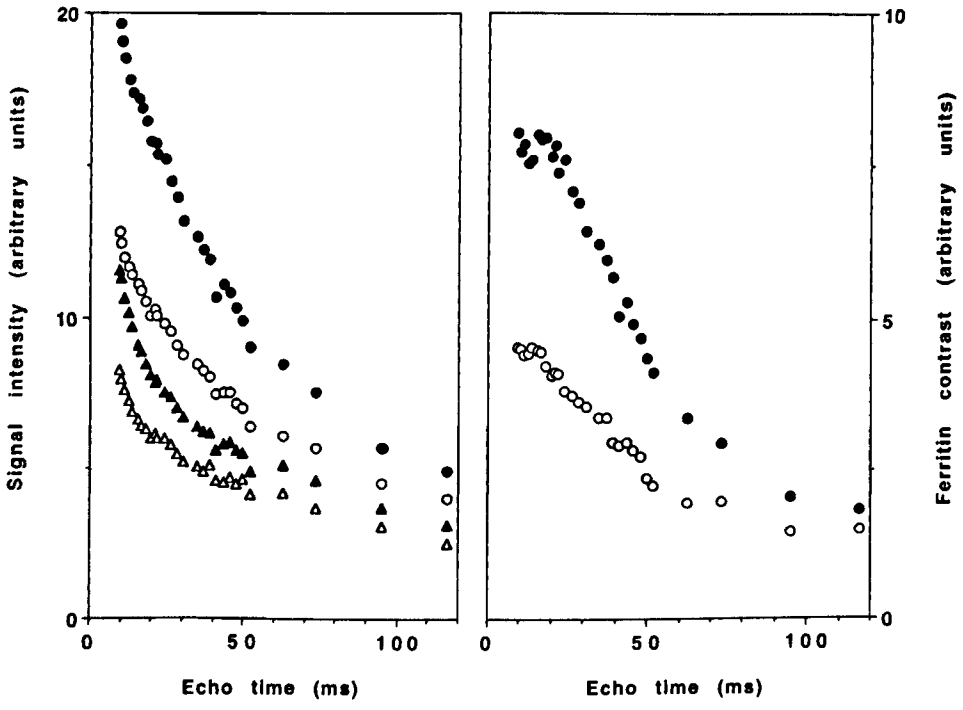

FIG. 6. Intensity and contrast effects of ferritin in *Xenopus* oocytes. (a) Mean signal intensity curves of animal (●, ▲) and vegetal (○) poles of ferritin-injected (▲) and apoferritin-injected (●, ○) oocytes. (b) Ferritin contrast in the animal pole (●) and vegetal pole (○). Maximal contrast was at minimal echo time for both animal (37% difference) and vegetal (32%) regions.

icantly lower in the ferritin-injected group. In all ferritin-injected oocytes, the nucleus T_{2a} was markedly shorter than that in apoferritin-injected oocytes.

DISCUSSION

The dominant mechanism of ferritin-induced water relaxation at high field is due to diffusion of water past the large magnetic field gradients. This mechanism of relaxation implies that magnetization can, in principle, be refocused (thus reducing ferritin contrast) by a CPMG pulse sequence if the gradients are not large relative to the τ_{CPMG} delay. Indeed, longer relaxation times and, therefore, lower ferritin-induced contrast were recently demonstrated for deoxy blood and also for the globus pallidum of a Rhesus monkey, at short τ_{CPMG} at a field of 1 T (17). In the study reported here, we found that ferritin contrast at 9.4 T was improved in images acquired with short τ_{CPMG}. Optimization of ferritin detection was done by varying the τ_{CPMG} duration of a spin-echo train from 5 ms down to 50 μs, thus shifting the apparent relaxation time from T_2 to $T_{1\rho}$. Ferritin relaxivity was not significantly affected by the variation in τ_{CPMG} duration. This finding is in accord with the short diffusion correlation time of ferritin, as compared to τ_{CPMG}. On the other hand, BSA-induced transverse relaxation was significantly lowered at short τ_{CPMG}. Analysis of the NMRD profile for BSA yielded a correlation time of 12 μs. Similar $T_{1\rho}$ NMRD profiles with comparable correlation times have been reported for gelatin (11) and protein solutions (18) as well as for excised tissue (11, 19). Through application of short τ_{CPMG}, ferritin-induced contrast could be enhanced by 35%.

Xenopus oocytes were imaged, using the short τ_{CPMG} imaging sequence. The two poles of the cytoplasm, as well as the nucleus, could be distinguished according to signal intensity, in accordance with previous reports (12, 13). The τ_{CPMG} duration had a dramatic effect on *Xenopus* oocyte transverse relaxation. Whereas at long durations signal intensity decayed to noise level within about 20 ms, as reported previously (12, 13), a short τ_{CPMG} duration (100 μs) allowed collection of data points up to 120 ms. In accordance with the results of the BSA solutions, this indicates a significant contribution of diamagnetic, rather than paramagnetic, mechanism to transverse relaxation. *Xenopus* oocyte transverse relaxation, in contrast to the ferritin, apoferritin, and BSA solutions, did not follow a single exponential decay curve. Biexponential analysis revealed a short cytoplasmic T_2 of approximately 20 ms and a long one of approximately 100 ms.

Injection of apoferritin into the *Xenopus* oocyte cytoplasm had no significant effect on transverse relaxation. Ferritin (about 1 mg/ml cytoplasmic concentration), on the other hand, caused a marked increase in transverse relaxation. Cytoplasmic signal intensity of ferritin-injected oocyte was more than 30% lower than that of control oocytes at minimal echo time. Maximal ferritin contrast was found at the minimal echo time. Biexponential relaxation analysis showed that whereas the short term dropped by approximately 6 ms in ferritin-injected oocytes, the long term was not significantly affected. A similar biexponential relaxation was recently reported for *Xenopus* oocytes by Pauser *et al.* (20).

The mechanism of water relaxation enhancement by ferritin could be deduced from the dependence on iron loading. The quadratic dependence of transverse relaxivity on the loading factor is in accord with a paramagnetic mechanism, as outlined in the Introduction. The additional zero order offset cannot be explained by paramagnetism. The expected magnetic moment $<\mu>$ of a paramagnetic ion in an external magnetic field can be found by weighing its allowed angular momentum components along the field's axis according to the Boltzman distribution. Assuming an ideal ground state core of ferric ions ($S = J = 5/2$) in a magnetic field of 9.4 T at room temperature and a core loaded with 1000 Fe^{3+} ions implicates about 50 moments aligned with the field, each equal to 5 Bohr Magnetons. According to Gauss's theorem, these could all be considered to be at the center of the ferritin complex, each contributing a field of approximately 2.12 G at the protein surface. The total field inhomogeneity at the equator would be about 0.45 MHz. For 1 mg/ml of ferritin, the volume fraction from which the solvent is excluded is approximately 0.15%. Taking a correlation time ($\tau = R^2/D$) of approximately 2.1×10^{-8} s ($r = 130$ Å and $D = 2 \times 10^{-5}$ cm^2/s), the predicted value for the quadratic loading factor coefficient would be 7.6×10^{-7} [$s^{-1} \times$ (loading factor)$^{-2}$/mg/ml protein], in very good agreement with the experimental value of 8 ($\pm$ 0.9) $\times$ 10^{-7} [$s^{-1} \times$ (loading factor)$^{-2}$/mg/ml protein]. The quadratic contribution of ferritin relaxivity could, therefore, be well attributed to a regular paramagnetic mechanism at high field.

The paramagnetic contribution to relaxivity should be quadratically dependent on the magnetic field strength. At a field of 20 MHz (8), the paramagnetic contribution would be about 2×10^{-3} s^{-1} for a core loaded with 1000 Fe^{3+} ions, negligible compared to the reported ferritin relaxivity of approximately 0.5 s^{-1}/mg/ml of protein. The high relaxivity measured at low field may be related to the zero order term found here. The zero order term of 2.7 [s^{-1}/mg/ml of protein] does not correspond to the paramagnetic character of the iron core and was significantly larger than any apparent experimental error. One source for this term could be dipolar interactions between bound iron ions and bound protons in their vicinity, as reported for the effect of ferritin on T_1 of water (8). This contribution is on the order of 0.2 s^{-1}/mg/ml of protein at 0.02–20 MHz, is partly dispersive in nature, and will not significantly affect outer sphere relaxation. Thus, the expected contribution to transverse relaxation at 400 MHz should be small. Another possible contribution may be due to ferromagnetic domains created during the initial stages of the formation of the iron core by imperfect oxidation of ferrous ions with regions of mixed valence. This second hypothesis is in accord with the fact that the specific relaxivity at 20 MHz, reported by Vymazel *et al.* (9), was very similar to that reported by Koenig *et al.* (8), despite a 2.5-fold difference in the loading factor. Thus, it seems that the initial stages of the iron core loading are responsible for the anomalous transverse relaxivity properties of ferritin and are manifested in a high field by the zero order term.

In conclusion, the effect of ferritin iron loading on water transverse relaxivity points to a paramagnetic mechanism as the main contributor in a high magnetic field. This effect, however, should be proportional to the square of the field and, thus, at a field of 4 T, the paramagnetic effect will be of the same order as the zero order term. One consequence of this would be that for a given tissue iron content, at imaging fields lower than 4 T, a larger number of ferritin complexes with lower iron loading will enhance water relaxation more effectively than a smaller number of complexes with higher loading factors. Ferritin loading factor in biological tissue is distributed around a mean value of approximately 1000 iron ions per core (2). The loading factor *in vivo* could perhaps be experimentally modulated in transgenic animals with controlled expression and translation of apoferritin. The significant ferritin contrast obtained in the *Xenopus* oocyte demonstrates the advantage of a short τ_{CPMG} or a spin-lock sequence over a single spin echo. However, ferritin contrast *in vivo* may be even larger, using T_2*-sensitive sequences, due to susceptibility differences between regions containing different amounts of ferritin (21).

ACKNOWLEDGMENTS

The authors thank Professor Nathan Daskal for his help in preparation and for microinjections of *Xenopus* oocytes and Professor Z. Luz for helpful discussions.

REFERENCES

1. S. Levi, A. Luzzago, G. Cesareni, A. Cozzi, F. Franceschinelli, A. Albertin, P. Arosio, Mechanism of ferritin iron uptake: activity of the H-chain and deletion mapping of the ferro-oxidase site. *J. Biol. Chem.* **263,** 18086–18092 (1988).
2. P. M. Harrison, T. H. Lilley, Ferritin, *in* "Physical Bioorganic Chemistry Series: Iron Carriers and Iron Proteins" (T. M. Loehr, Ed.), pp. 125–238, Weinheim, VCH, 1989.
3. C. M. Morris, J. M. Candy, A. B. Keith, A. E. Oakley, G. A. Taylor, R. G. L. Pullen, C. A. Bloxham, A. Gocht, J. A. Edwardson, Brain iron homeostasis. *J. Inorg. Biochem.* **47,** 257–265 (1992).
4. J. R. Connor, S. L. Menzies, S. M. St. Martin, E. J. Mufson, Cellular distribution of transferrin, ferritin, and iron in normal and aged human brains. *J. Neurosci. Res.* **27,** 595–611 (1990).
5. J. C. Chen, P. Hardy, W. Kucharczyk, M. Clauberg, J. G. Joshi, A. Vourlas, M. Dahr, R. M. Henkelman, MR of human postmortem brain tissue: correlative study between T_2 and assays of iron and ferritin in Parkinson and Huntington disease. *Am. J. Neuroradiol.* **14,** 275–281 (1993).
6. C. Schenker, D. Meier, W. Wichmann, P. Boesiger, A. Valavanis, Age distribution and iron dependency of the T_2 relaxation time in the globus pallidus and putamen. *Neuroradiology* **35,** 119–124 (1993).
7. R. J. Ordidge, J. M. Gorell, J. C. Deniau, R. A. Knight, J. A. Helpern, Assessment of relative brain iron concentrations using T_2-weighted and T_2*-weighted MRI at 3 Tesla. *Magn. Reson. Med.* **32,** 335–341 (1994).
8. S. H. Koenig, R. D. Brown, J. F. Gibson, R. J. Ward, T. J. Peters, Relaxometry of ferritin solutions and the influence of the Fe^{3+} core ions. *Magn. Reson. Med.* **3,** 755–767 (1986).
9. J. Vymazel, R. A. Brooks, O. Zak, C. McRill, C. Shen, G. Di Chiro, T_1 and T_2 of ferritin at different field strengths: effect on MRI. *Magn. Reson. Med.* **27,** 368–374 (1992).
10. P. Gillis, S. H. Koenig, Transverse relaxation of solvent protons induced by magnetized spheres: application to ferritin, erythrocytes, and magnetite. *Magn. Reson. Med.* **5,** 323–345 (1987).
11. G.E Santyr, R. M. Henkelman, M. J. Bronskill, Variations in measured transverse relaxation in tissue resulting from spin locking with the CPMG sequence. *J. Magn. Reson.* **79,** 28–44 (1988).
12. J. B. Aguayo, S. J. Blackband, J. S. Schoeniger, M. A. Mattingly, M. Hintermann, Nuclear magnetic resonance imaging of a single cell. *Nature* **322,** 190–191 (1986).
13. S. Posse, W. P. Aue, Spectroscopic imaging and gradient-echo microscopy on a single cell. *J. Magn. Reson.* **83,** 620–625 (1989).
14. S. Pauser, K. Keller, A. Zschunke, C. Mugge, Study of the membrane permeability of a paramagnetic metal complex on single cells by NMR microscopy. *Magn. Reson. Imaging* **11,** 419–424 (1993).
15. M. M. Bradford, A rapid and sensitive method for quantitation of microgram quantities of protein utilizing the principles of protein-dye binding. *Anal. Biochem.* **72,** 248–254 (1976).
16. N. Dascal, The use of *Xenopus* oocytes for the study of ion channels. *Crit. Rev. Biochem.* **22(4),** 317–387 (1987).
17. R. A. Brooks, J. Vymazal, J. W. M. Bulte, C. D. Baugarner, V. Tran, Comparison of T2 relaxation in blood, brain, and ferritin. *J. Magn. Reson. Imaging* **4,** 446–450 (1995).
18. S. H. Koenig, W. E. Schillinger, Nuclear magnetic relaxation dispersion in protein solutions. I. Apotransferrin. *J. Biol. Chem.* **244,** 3283–3289 (1969).
19. R. R. Knispel, R. T. Thompson, M. M. Pintar, Dispersion of proton spin-lattice relaxation in tissues. *J. Magn. Reson.* **14,** 44–51 (1974).
20. S. Pauser, A. Zschunke, A. Khuen, K. Keller, Estimation of water mobility in the nucleus and cytoplasm of *Xenopus laevis* oocytes by NMR microscopy. *Magn. Reson. Imaging* **13,** 269–276 (1995).
21. F. Q. Ye, P. S. Allen Ferritin as a susceptibility agent, *in* "Proc., SMRM, 12th Annual Meeting, New York, 1993," p. 800.